Carbohydrate Polymers 115 (2015) 177–185

Contents lists available at ScienceDirect

Carbohydrate Polymers

journal homepage: www.elsevier.com/locate/carbpol

Removal of cadmium(II) from aqueous solutions by chemically modified maize straw

Hong Guo [a,b], Shufen Zhang [a,*], Zinong Kou [c], Shangru Zhai [b], Wei Ma [a], Yi Yang [b]

[a] State Key Lab of Fine Chemicals, Dalian University of Technology, Dalian 116024, China
[b] Faculty of Light Industry and Chemical Engineering, Dalian Polytechnic University, Dalian 116034, China
[c] Instrument Analysis Centre, Dalian Polytechnic University, Dalian 116034, China

ARTICLE INFO

Article history:
Received 26 March 2014
Received in revised form 5 August 2014
Accepted 9 August 2014
Available online 27 August 2014

Keywords:
Maize straw
Succinylation
Adsorption
Cadmium

ABSTRACT

A new regenerable adsorbent was successfully prepared by modifying maize straw (MS) with succinic anhydride in xylene. The succinylated-maize straw (S-MS) was characterized by FTIR, solid-state MAS ^{13}C NMR spectroscopy, SEM-EDX and point of zero charge analysis. NaS-MS was successfully obtained after deprotonating the carboxylic acid groups of S-MS by Na_2CO_3 solution. Batch experiments were carried out with NaS-MS for the removal of Cd(II). The effects of pH, adsorbent dosage, contact time, initial concentration and temperature were investigated. The experimental data were best described by a pseudo-second-order kinetics and Langmuir adsorption models. Thermodynamic parameters (ΔG, ΔH, and ΔS) were also calculated from data obtained from experiments performed to study the effect of temperatures. NaS-MS could be regenerated at least five times in saturated NaCl solution without any loss. Furthermore, ~97% of adsorbed Cd(II) ions could be recovered as the metal oxide. Finally, the adsorption mechanism of NaS-MS was discussed.

1. Introduction

Water pollution with heavy metals has become an increasing public concern in recent decades. Among the metals, cadmium is particularly regarded as one of the most hazardous substances. It is introduced into water from metal plating, cadmium nickel batteries, and alloys, all of which are products of industrial activities. Unlike organic pollutants which are susceptible to biological degradation, cadmium accumulates in vital organs in humans and animals, thereby posing a great danger to living organism (Çay, Uyanık, & Özaşık, 2004). Thus, development of treatment methods that facilitate the removal of cadmium from wastewaters, prior to their discharge into natural water system, is in great demand.

Several methods have been developed to remove cadmium from wastewaters. Activated carbons (Macías-García, Gómez-Serrano, Alexandre-Franco, & Valenzuela-Calahorro, 2003), ion exchangers (Kaušpedienė, Snukiškis, & Gefenienė, 2003), and complexing agents made from natural and synthetic reagents (Abou-Mesalam, 2003; Malla, Alvarez, & Batistoni, 2002) are commonly used in these methods. Although these absorbents showed excellent adsorption capacity toward cadmium, they incurred high costs and generated poisonous reaction byproducts. Recently, much attention has been diverted to the use of inexpensive and effective ion exchangers produced from agricultural wastes.

Maize straw (MS) is one of the major agriculture wastes, and estimated that about 250 million tons are produced annually in China (Chen, Zhao, & Xia, 2008). It is not used as industrial raw material but incinerated or abandoned, thus the disposal of maize straw has been considered as a significant problem. Interestingly, MS is predominantly composed of cellulose (28.4–37.7%), hemicelluloses (25.7–25.4%), and lignin (16.7–18.9%) (Wang, Guo, & Guo, 2006). The large amount of easily available hydroxyl groups allow for a series of chemical reactions, such as esterification, etherification, and copolymerization, thus making MS a suitable candidate for conversion to an adsorbent. It has been reported that the vicinal carboxyl groups of succinate, separated by a single bond, can rotate freely to accommodate large cations (Lehrfeld, 1996). In recent decades, several researchers have modified agriculture wastes, such as olive stone (Aziz, Elandaloussi, Belhalfaoui, Ouali, & Ménorval, 2009), pineapple peel (Hu, Zhao, & Huang, 2010), babassu coconut mesocarp (Vieira et al., 2010), corncob (Clave et al., 2004), and posidonia (Chadlia, Mohamed, Najah, & Farouk, 2009), with succinic anhydride for use as adsorbents in the removal of heavy metal ions. To the best of our knowledge, the modification of MS with succinic anhydride and its potential for heavy metal adsorption have not been reported till now.

* Corresponding author. Tel.: +86 411 84986265; fax: +86 411 84986264.
E-mail address: zhangshf@dlut.edu.cn (S. Zhang).

http://dx.doi.org/10.1016/j.carbpol.2014.08.041
0144-8617/

Therefore, in this study, MS was first modified with succinic anhydride for the introduction of carboxylic groups; subsequently, the carboxylates in the product (S-MS) were treated with Na_2CO_3 to generate the sodium salt of the carboxylates (NaS-MS). Then, NaS-MS was used in the removal of Cd(II) from an aqueous solution. The influence of various experimental parameters, such as pH, adsorbent dosage, initial concentration, contact time, isotherms, and temperature has been investigated. Furthermore, the regenerability of NaS-MS and the recovery of the adsorbed Cd(II) were also examined. Finally, the adsorption mechanism was systematically investigated.

2. Materials and methods

2.1. Materials

Maize straw (MS) was obtained from Dalian, China, and then cut into 10 cm length pieces. The cut straw was further treated with 10% NaOH for 2 h at room temperature to remove impurities. After filtering, the solid was washed with distilled water till the effluent was neutral. The solid was then dried at 353 K in hot air oven until it maintained a constant weight. Stock solution of cadmium chloride was made by dissolving $CdCl_2{\cdot}2.5H_2O$ in distilled water and test solutions of descried concentrations were obtained by further dilution with distilled water. All chemicals and solvents used were analytical grade and used without further treatment or purification.

2.2. Preparation of S-MS and NaS-MS

The washed and dried MS (0.5 g) was suspended in a mixture of succinic anhydride (1.0 g) and xylene (50 mL). Triethylamine (1.4 mL, equi-molar to succinic anhydride) was added to the solution. The solution was refluxed for 8 h. After cooling to room temperature, the solution was filtered and the solid was washed thoroughly with acetone and water to remove the unreacted succinic anhydride. The resulting light-yellow solid (0.90 g) was designated as S-MS.

S-MS was treated with sodium carbonate solution (0.01 mol L^{-1}) for 1 h under constant stirring at 293 ± 2 K and then filtered. The solid was washed with distilled water till the pH of the washings was neutral. The solid, designated NaS-MS, was then dried in an oven at 378 K for 4 h and passed through a 0.5 mm sieve.

2.3. Analysis of lignin

The content of acid-soluble lignin and acid-insoluble lignin in MS or S-MS was measured according to TAPPI T222.

2.4. Degree of succinylation

The degree of succinylation of MS was determined by measuring the quantity of introduced acid function. And the carboxylic content of S-MS was determined by the back titration method (Jr et al., 2007). 0.1 g of S-MS was treated with 100 mL 0.01 mol L^{-1} NaOH standard solution by stirring at room temperature for 1 h. Soon thereafter the materials were separated by single filtration. Several drops of phenolphthalein indicator were added. The above solution was back titrated against 0.01 mol L^{-1} standard HCl solution until the solution turned from the pale pink to colorless. The carboxylic content of S-MS (C_{COOH}, mmol g^{-1}) was calculated by Eq. (1):

$$C_{COOH} = \frac{V_{NaOH} * C_{NaOH} - V_{HCl} * C_{HCl}}{m_{S\text{-}MS}} \quad (1)$$

where, V_{NaOH} (mL) and V_{HCl} (mL) are the volume of standard NaOH used and standard HCl consumed, respectively. C_{NaOH} (mmol L^{-1}) is the concentration of the NaOH solution, C_{HCl} (mmol L^{-1}) is the concentration of the HCl solution, and $m_{S\text{-}MS}$ (g) is the S-MS mass.

2.5. Characterization

The functional groups present in MS and S-MS were characterized by Fourier transform infrared (FTIR, Perkin-Elmer, USA) and cross polarization magic angle spinning (CPMAS) ^{13}C NMR spectrometer (Bruker AVANCE III 600, Germany). The surface morphologies of MS and S-MS were visualized in a JEOL JSM-6460LV field emission SEM, equipped with an energy dispersive X-ray spectroscope (Oxford, British). The pH at the point of zero charge (pH_{PZC}) of S-MS was determined by the solid addition method (Kiefer, Sigg, & Schosseler, 1997).

2.6. Adsorption experiments

Batch adsorption experiments were carried out for 1.5 h in 100 mL Erlenmeyer flasks containing a magnetic stirrer at 150 rpm of Cd(II) (150 mg L^{-1}, 50 mL). After stirring, the samples were filtered through a 0.45 μm membrane filter and the residual Cd(II) concentration in the filtrate was determined by flame atomic adsorption spectrophotometer (FAAS HITACHI 180-80, Japan) equipped with air–acetylene flame. The amount of adsorption at equilibrium q_e (mg g^{-1}) and the percentage removal efficiency (%R) were calculated according to Eqs. (2) and (3):

$$q_e = \frac{(C_0 - C_e)V}{W} \quad (2)$$

$$\%R = \frac{C_0 - C_e}{C_0} * 100\% \quad (3)$$

where C_0 and C_e are the initial and equilibrium solution concentrations of Cd(II) (mg L^{-1}), respectively. V (L) is the volume of the solution, and W (g) is the weight of the used adsorbent, and q_e is the equilibrium adsorption capacity (mg g^{-1}). During the adsorption process, dependence of the initial concentration, adsorbent dose, contact time, temperature, and pH on the adsorption behavior was investigated thoroughly. The corresponding supernatants were immediately centrifuged, collected, and diluted for concentration analysis by FAAS.

2.7. Regeneration and recovery

2.7.1. Regeneration experiments

The regeneration of NaS-MS was carried out at 293 ± 2 K. First, NaS-MS (1 g L^{-1}) was subjected to Cd(II) adsorption in a solution of Cd(II) (150 mg L^{-1}). After 1.5 h of contact time, the suspension was filtered and the Cd(II) concentration in the filtrate was determined by FAAS. The recovered solid was washed with distilled water, air dried, and suspended in saturated sodium chloride solution (100 mL). The obtained suspension was stirred for 1.5 h, centrifuged, and the supernatant was analyzed by FAAS. The regenerated material was washed with distilled water until the test with $AgNO_3$ for the presence halide was negative. Five sequential cycles of adsorption–desorption were carried out.

2.7.2. Recovery of adsorbed Cd(II) as oxide

NaS-MS, after being shaken in a solution of Cd(II) for 1.5 h, was collected by filtration and transferred to a porcelain crucible, then they were put into a muffle furnace and heated for 8 h at high temperature (873 K) to convert the adsorbed Cd(II) to its oxide. Its structure was investigated by X-ray diffraction (XRD, SHIMADZU XRD-6100, Japan). After cooling the crucible to room temperature, hydrochloric acid (1 mol L^{-1}, 10 mL) was added to dissolve the

metal oxide. The concentration of dissolved Cd(II) was determined by FAAS to calculate the recovery percentage.

3. Results and discussion

3.1. Synthesis of S-MS

Alkali treatment of natural fibers, also called mercerization, is the common method to produce high-quality fiber, for this method can increase the number of possible reaction sites and remove some cementing substances in the fibers such as lignin and hemicellulose (Kalia, Kaith, & Kaur, 2009). When MS is treated with NaOH, most of the lignin is removed. Lignin is a polyfunctional polymer with a three-dimensional structure which renders the raw material less inclined toward functionalization (Belhalfaoui, Aziz, Elandaloussi, Ouali, & Ménorval, 2009). The concentrations of lignin in MS and mercerized MS are 18.2% and 4.5%, respectively, which indicates that mercerization can improve the reactivity of raw material.

The protocol for the synthesis of S-MS and NaS-MS is shown in Scheme S1. The hydroxyl groups in MS were treated with succinic anhydride to yield the stable ester and free carboxylic acid end groups, thereby increasing the number of adsorption sites on the surface of MS for metal cations. Since the esterification reaction can be catalyzed by an acid or base, the weak base triethylamine is used here. Triethylamine is an excellent catalyst and ensures that 70% of the succinic anhydride is consumed. Sodium carbonate offers a mildly basic condition to deprotonate the free carboxylic acid groups and converts them to their sodium salts (NaS-MS) without destroying the ester bond.

3.2. Characterization

The modification of MS by succinic acid was confirmed by FTIR spectroscopy. Fig. 1 shows the FTIR spectra of MS and S-MS. Three major differences between the two spectra can be observed. First, the peak at 1746 cm^{-1} in the S-MS spectrum corresponds to the absorption of carbonyl bonds of both esters and carboxylic acid groups. Second, the emergence of the band in the 3435 cm^{-1} in the S-MS spectrum can be ascribed to the O—H stretching bands of the terminal carboxylic acids. And lastly, the increase and decrease in the intensities of the absorption bands at 1167 cm^{-1} and 1058 cm^{-1} for S-MS can be attributed to C—O asymmetric stretching and C—O—C band stretching, respectively. These changes confirm the succinylation of MS; one of the carboxylates is involved in the ester bond with hydroxyls on the surface of MS while the other (as a carboxylic acid) is dangling free (Aziz et al., 2009).

Fig. 2 shows the MAS ^{13}C NMR spectra of MS and S-MS. The signals in the region between 50 ppm and 105 ppm, specific for the carbons in carbohydrates, are similar in both the spectra. The presence of the signals typical for the carboxylic group at 173 ppm and for the methylene group at 29 ppm in the spectra of S-MS is the evidence of succinoylation. Similar observations have been reported by others for the esterification of sugarcane bagasse (Liu et al., 2008).

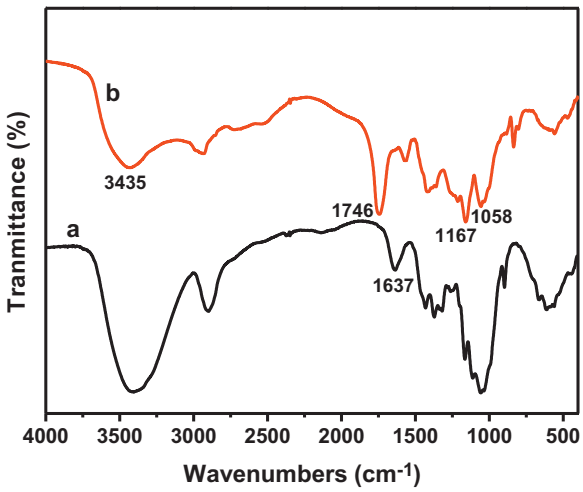

Fig. 1. FTIR spectra of MS (a) and S-MS (b).

The surface morphologies of MS and S-MS are shown in Fig. 3. It is obvious that the surface of S-MS is smoother in comparison with that of MS, which indicates that the grafted carboxylic groups nearly homogenously cover the surface of the fibers.

As shown in Fig. S1, the pH_{PZC} values of MS and S-MS are determined to be 7.4 and 5.4, respectively. The pH_{PZC} shifts to a lower pH value because of the introduction of acidic surface groups. Furthermore, the titration of carboxylic acid groups gives the concentration of carboxylic functions (n_{COOH}) value of 4.2 mmol g^{-1}.

3.3. Adsorption of cadmium

3.3.1. Effect of pH on the removal of cadmium by S-MS and NaS-MS

The pH of the initial solution, which determines both the nature of the metallic species and the charge on the adsorbent surface (Zhang et al., 2013), is one of the most important parameters affecting the sorption process. In order to illuminate the sorption mechanism, the sorption tests should be performed at the optimum pH zone. Stability constants of Cd(II) have been provided by Srivastava, Mall, and Mishra (2008). When the pH value is < 7,

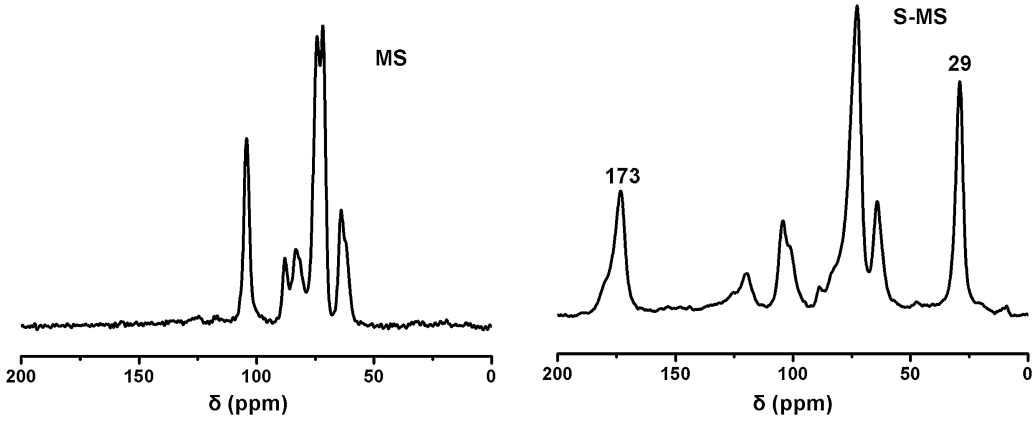

Fig. 2. MAS ^{13}C NMR spectra of MS and S-MS.

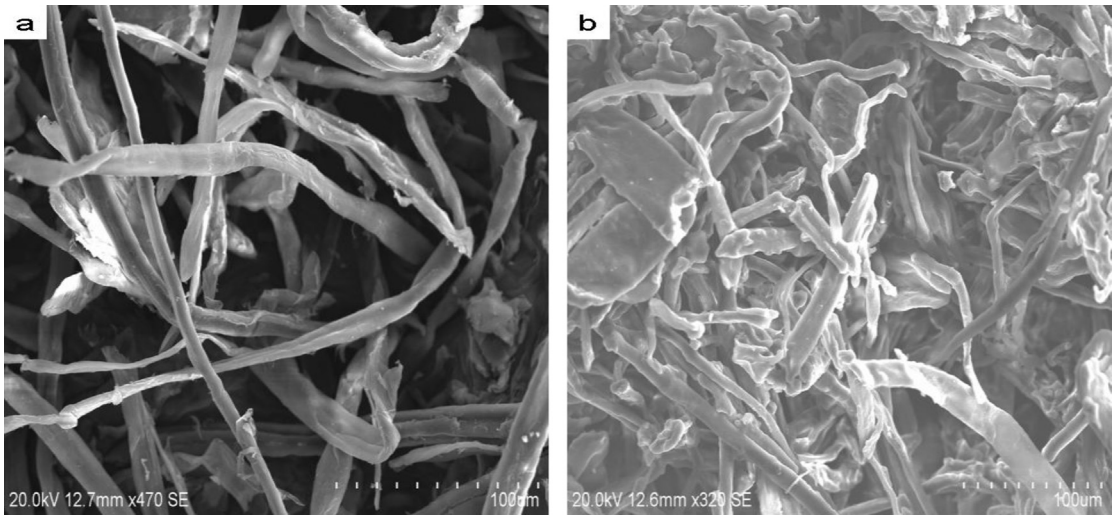

Fig. 3. SEM micrographs of MS (a) and S-MS (b).

Cd(II) exists mainly in the ionic state, i.e., divalent Cd^{2+}. The precipitation of $Cd(OH)_2$ and other Cd(II) species such as $Cd(OH)^+$ and $Cd(OH)^{3-}$ does not occur until the pH value is > 7. Accordingly, to avoid the simultaneous precipitation of $Cd(OH)_2$ and the adsorption of $Cd(OH)^+$, the experiments were carried out at pH values between 2 and 6.

Fig. 4a displays the effect of the initial pH (pH_i) on the adsorption behaviors of MS, S-MS, and NaS-MS. Cd(II) was hardly adsorbed by MS. The adsorption capacity of MS was much lower than that of S-MS and NaS-MS and was not affected by the value of pH_i. The results indicate that the carboxyl groups anchored onto the MS play an important role in the adsorption of Cd(II). As illustrated in Fig. 4a, the adsorption capacities of S-MS and NaS-MS increase significantly as the pH_i increased from 2.0 to 4.0, however, with further increase in pH_i from 4.0 to 6.0, the adsorption capacity is maintained at a constant level. pH_{PZC} determines the combined influence of the functional groups of surface. The pH_{PZC} for S-MS is 5.4, which means that the adsorbent surface is positively charged when pH < 5.4 (Fig. S1). The surface is negatively charged when the pH > 5.4 and favors the adsorption of cations.

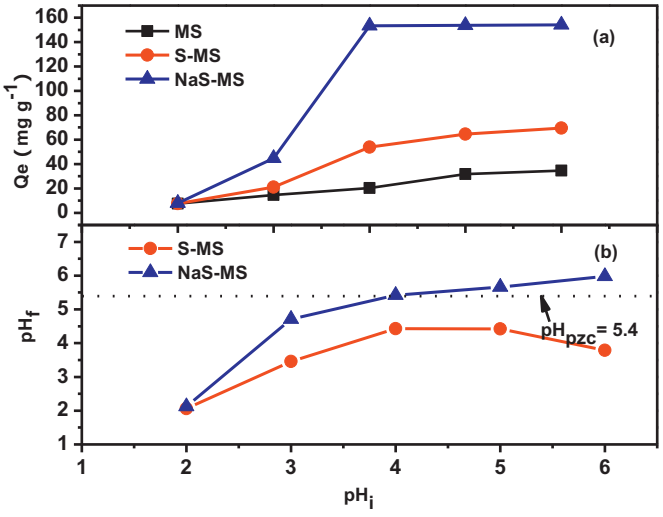

Fig. 4. Effect of pH_i on the removal of cadmium(II) for MS, S-MS and NaS-MS (panel a), pH changes during the cadmium adsorption process by S-MS and NaS-MS (panel b), (C_0 = 150 mg L^{-1}, adsorbent dose = 1 g L^{-1}, T = 293 ± 2 K, t = 1.5 h).

To investigate the adsorption mechanism, it is necessary to detect the pH of the solution during the adsorption. The final pH values (pH_f) of the sorption process are shown as a function of pH_i in Fig. 4b. When the value of pH_i < 4.0, the pH_f values of the solution after adsorption by S-MS and NaS-MS are lower than that of the corresponding $pH_{PZC's}$ (Fig. 4b). Consequently, a significant electrostatic repulsion exists between the positively charged surface of the adsorbents and Cd(II). For $pH_i \geq 4.0$, the pH_f value for the experiment with NaS-MS is higher than its pH_{PZC}, which leads to the deprotonation of positively charged groups on the adsorbent. This leads to an increase in the adsorption capacity of NaS-MS because of electrostatic attraction between negatively charged sites on its surface and Cd^{2+} ions. However, the adsorption capacity of S-MS is much lower than that of NaS-MS for $4.0 \leq pH_i \leq 6.0$, because the pH_f value when S-MS is used for adsorption is lower than pH_{PZC}. Since NaS-MS has a higher adsorption capacity than S-MS, subsequent Cd(II) adsorption experiments are performed with NaS-MS. As seen in Fig. 4a, the pH range for the optimal removal of Cd(II) by the adsorbents is 4.0–6.0; in this pH range, the precipitation due to the formation of $Cd(OH)_2$ is precluded. The pH of original Cd(II) solution (5.8) needs no adjustment in the subsequent experiments.

3.3.2. *Effect of adsorbent dose*

The effect of NaS-MS dosage on the adsorption of Cd(II) is studied by varying the concentration of the sorbent in the initial Cd(II) solution (pH = 5.8) (Fig. 5). The fraction of Cd(II) removal increases significantly from 42.5% to 96.3% when the amount of the adsorbent is increased from 0.2 to 1.0 g L^{-1}; with more number of adsorption sites available, the higher percentage of Cd(II) is removed (Bhattacharyya & Sharma, 2004). Beyond a critical dose (1 g L^{-1} in case of NaS-MS), the adsorption ability is almost unchanged. There is no significant decrease in the solution concentration of Cd(II) with any further increase in the concentration of NaS-MS (1 g L^{-1}). This is due to the saturation of the active sites on NaS-MS and the presence of residual amount of free Cd(II). However, the equilibrium adsorption capacity (q_e) decreases with the increase in adsorbent concentration. The adsorption capacity decreases from 320.5 mg g^{-1} to 121.2 mg g^{-1}, as the adsorbent concentration is increased from 0.2 to 1 g L^{-1} (Fig. 5). This result is attributed to the competition for Cd(II) between the adsorption sites (Baral, Das, Chaudhury, Swamy, & Rath, 2008). Similar behavior has also been reported in other systems (Chadlia et al., 2009). For industrial applications of NaS-MS, both the dose of adsorbent and the removal

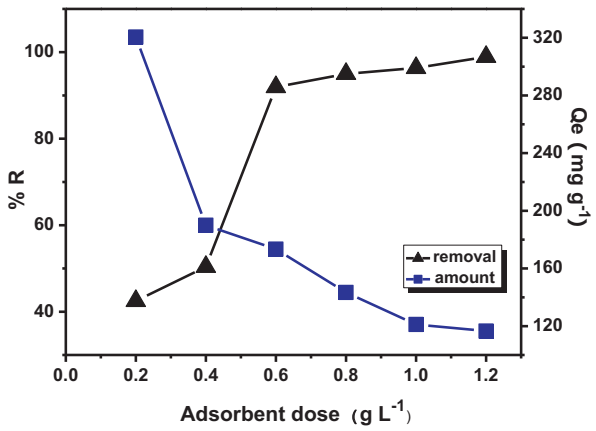

Fig. 5. Effect of adsorbent dose on the adsorption capacity and removal percentage of cadmium by NaS-MS (C_0 = 150 mg L^{-1}, original pH 5.8, T = 293 ± 2 K, t = 1.5 h).

efficiencies must be considered. Therefore, 1.0 g L^{-1} of adsorbent is chosen for all subsequent studies on Cd(II).

3.3.3. *Effect of contact time and initial cadmium concentration*

The amount of Cd(II) adsorbed (q_t) versus the contact time with various initial cadmium concentrations is shown in Fig. 6a. The sorption process is fast in the initial stage; about 70.0%-96.6% of total Cd(II) in solution is removed within the first minute of contact. The fast adsorption process is associated with its activation energy, which is explained in Section 3.3.5. The subsequent slow step involves the rearrangement of the adsorbed Cd(II) on the surface and leads to a more thorough utilization of the adsorption sites in the adsorbent.

Fig. 6a also shows that the equilibrium adsorption capacity of NaS-MS increases from 95.43 mg g^{-1} to 197.62 mg g^{-1} with the increase initial Cd(II) concentrations from 100 mg L^{-1} to 500 mg L^{-1}. This can be explained by the fact that with increase in the initial concentration, the mass transfer driving force accelerates the diffusion of Cd(II) from the bulk solution onto adsorbent, hence resulting in higher adsorption capacity. The equilibrium time is independent of the initial Cd(II) concentration. Therefore, subsequent studies are carried out using a period of 1.5 h as a suitable contact time for Cd(II) adsorption.

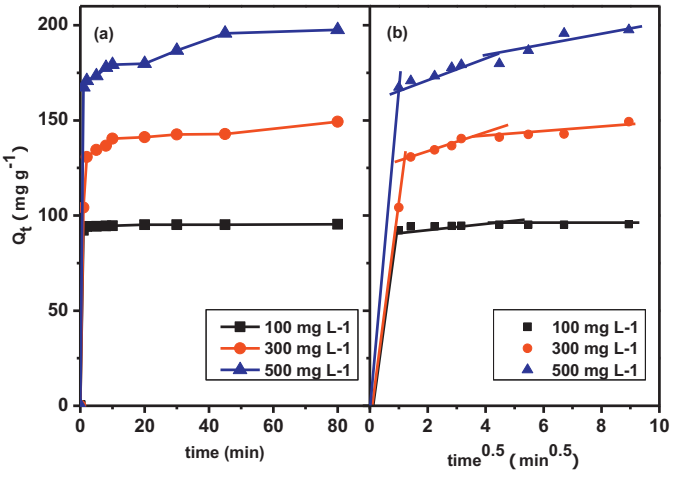

Fig. 6. Effect contact time on the adsorption capacity of cadmium(II) (panel a) and intraparticle diffusion plots (panel b) by NaS-MS (C_0 = 100, 300 and 500 mg L^{-1}, original pH 5.8, adsorbent dose = 1 g L^{-1}, T = 293 ± 2 K).

3.3.4. *Kinetics models of adsorption*

In order to determine the mechanism of Cd(II) adsorption by NaS-MS, several kinetic models such as the pseudo-first-order kinetics, pseudo-second-order kinetics, and intraparticle diffusion kinetics were employed to study the adsorption.

The linear pseudo-first-order model is given as follows (Eq. (4)):

$$\ln(q_e - q_t) = \ln\ q_e - k_1 t \tag{4}$$

where q_e and q_t are the adsorption capacity per unit weight of adsorbent (mg g^{-1}) at equilibrium and at time t (min), respectively, and k_1 is the pseudo-first-order rate constant (min^{-1}). The values of $\ln(q_e - q_t)$ are calculated from the experimental data and plotted against t, and the slope of the fitted linear curve gives the value of k_1.

The linear form of the pseudo-second-order equation is computed as Eq. (5):

$$\frac{t}{q_t} = \frac{1}{k_2 q_e^2} + \frac{t}{q_e} \tag{5}$$

Here k_2 is the pseudo-second-order rate constant (g mg^{-1} min^{-1}). The values of t/qt are plotted against t, and the predicted adsorption capacity q_e (mg g^{-1}) and k_2 are calculated from the slope and intercept of the plot, respectively.

When the experimental data are fitted with the pseudo-first-order kinetics, the correlation coefficients (R^2) are very low. In contrast, R^2 for the pseudo-second-order are high ($R^2 > 0.99$) and the calculated q_e values agree well with experimental values (Table 1). Thus, it can be concluded that the adsorption of Cd(II) on NaS-MS follows the pseudo-second-order kinetic model wherein the rate-limiting step is assumed to be chemical adsorption involving valence force through exchange or sharing of electrons between Cd(II) and adsorbent.

It can be observed from Table 1 that the pseudo-second-order rate constant k_2 decreases with an increase in initial Cd(II) concentration. An explanation for this observation is that the relative number of vacant and easily accessible adsorption sites are reduced with the increase in the initial Cd(II) concentrations. As a result, it takes more time to reach equilibrium and hence the observed reduction in the adsorption rate (Ramakrishna & Sulochana, 2009).

The mechanism of diffusion of the adsorbed Cd(II) from the adsorption sites on the surface to those available in the interior is analyzed in terms of the intraparticle diffusion model. According to the theory proposed by Weber and Morris (1963), the intraparticle diffusion model is expressed as follows (Eq. (6)):

$$q_t = k_{id} t^{1/2} + Z \tag{6}$$

where k_{id} is the intraparticle diffusion rate constant (mg g^{-1} $min^{-1/2}$) and Z is the constant (mg g^{-1}) that gives information about the thickness of the boundary layer, i.e., the larger the value of Z, the greater the effect of the boundary layer (Vimonses, Lei, Jin, Chow, & Saint, 2009). According to this model, if the plots of q_t as a function of $t^{1/2}$ are linear, and pass through the origin, the rate-limiting process is the only rate-limiting step.

As shown in Fig. 6b, the intraparticle diffusion plots for NaS-MS exhibit multilinearity, indicating that the intraparticle diffusion is not the only rate controlling step. Three stages are involved in the adsorption process. The first linear portion (sharpest) is the adsorption onto the external surface or the instantaneous adsorption stage. The second stage describes the gradual adsorption of Cd(II) and where the intraparticle diffusion is the rate-limiting step. The values of k_{id} and Z obtained from this portion linear analysis are listed in Table 1. With initial Cd(II) concentrations of 100, 300, and 500 mg L^{-1}, both k_{id} and Z increase with the increase in initial concentration, which reflects the increase in the thickness of boundary layer (Wang et al., 2010) and the decrease in the chance of external mass transfer. Hence, the chance of internal mass transfer

Table 1
Kinetic parameters for the adsorption of Cd(II) by NaS-MS at different initial concentrations (C_0 = 100, 300 and 500 mg L^{-1}, original pH 5.8, adsorbent dose = 1 g L^{-1}, T = 293 ± 2 K).

C_0 (mg L^{-1})	q_e(exp) (mg g^{-1})	Pseudo-second-order model			Intraparticle diffusion model		
		k_2 (g mg^{-1} min^{-1})	q_{cal} (mg g^{-1})	R^2	k_{2id}	Z	R^2
100	95.4	0.1575	95.2	1	0.3168	93.7	0.9879
300	149.3	0.0088	149.3	0.99	5.1681	123.1	0.9566
500	197.6	0.0053	200.0	0.99	5.2744	162.5	0.9804

is increased (Khaled, Nemr, El-Sikaily, & Abdelwahab, 2009). The last stage is the state of dynamic equilibrium between adsorbate adsorption and desorption. Other studies have reported similar findings (Gusmão, Gurgel, Melo, & Gil, 2012).

3.3.5. Sorption activation energy

Fig. S2 depicts effects of temperature on the adsorption capacity of cadmium ion by NaS-MS. The sorption capacity slightly increased with increasing temperature from 313 K to 318 K. According to Arrhenius equation, activation energy of the adsorption (E_a, J mol^{-1}) can be calculated using the following equation (Liu et al., 2013):

$$\ln \frac{k(T_2)}{k(T_1)} = \frac{E_a}{R}\left(\frac{1}{T_1} - \frac{1}{T_2}\right) \quad (7)$$

where k is the apparent rate constant, E_a is the activation energy, R is the gas constant (8.314 J mol^{-1} K^{-1}), and T is the temperature (K). The pseudo-second-order rate constant (k) and the predicted adsorption capacity (q_e) are summarized in Table S1. The magnitude of activation energy may give an idea about the type of sorption. Activated chemical adsorption means that the rate varies with temperature according to finite activation energy (8.4–83.7 kJ mol^{-1}). In nonactivated chemical adsorption, the activation energy is near zero (Aksu, 2002). According to the parameters of pseudo-second-order kinetic model, the energy of activation (E_a) is calculated to be 4.7 kJ mol^{-1}. The value is near zero, which is the magnitude as nonactivated chemical sorption. The low value of E_a suggests that the energetic barrier against the adsorption of metal ion is easier to overcome; therefore, adsorption process occurs very rapidly.

3.3.6. Adsorption isotherms

The Cd(II) adsorption isotherm measured using NaS-MS shows a regular shape with a steep initial slope, clearly indicating that NaS-MS acts as a high efficacy adsorbent at low Cd(II) concentration (Fig. S3). The batch experimental data are applied to Langmuir and Freundlich isotherm equations.

Langmuir isotherm model assumes that a mono-molecular layer is formed on adsorption and there is no interaction between the adsorbed molecules (Aksu, 2002). This model is expressed as Eq. (8):

$$\frac{C_e}{Q_e} = \frac{C_e}{Q_{max}} + \frac{1}{Q_{max}K_L} \quad (8)$$

where C_e is the equilibrium concentration of the adsorbate (mg L^{-1}), Q_e is the amount of adsorbate adsorbed per unit mass of adsorbent at equilibrium (mg g^{-1}), Q_{max} is the theoretical maximum monolayer adsorption capacity of the adsorbent (mg g^{-1}), and K_L is the Langmuir isotherm constant related to the adsorption energy (L mg^{-1}).

Moreover, the essential characteristics of the Langmuir isotherm can be used to predict whether the adsorption is favorable or unfavorable in terms of a dimensionless constant separation factor given as Eq. (9):

$$R_L = \frac{1}{1 + K_L C_0} \quad (9)$$

where K_L is the Langmuir constant and C_0 is the initial adsorbate concentration. $R_L > 1$ for unfavorable adsorption, $R_L = 1$ for linear adsorption, $0 < R_L < 1$ for favorable adsorption, and $R_L = 0$ for irreversible adsorption.

As another typical simulation model for adsorption, the Freundlich isotherm is often used for non-ideal adsorption that involves heterogeneous surface energy system. It is described as Eq. (10):

$$Q_e = K_F C_e^{1/n} \quad (10)$$

where K_F (L mg^{-1}) is the Freundlich adsorption constant, and $1/n$ is a measure of the adsorption intensity that determines whether the adsorption intensity and type of isotherm is favorable ($0.1 < 1/n < 0.5$) or unfavorable ($1/n > 2$).

The fitting parameters derived from Langmuir and Freundlich adsorption isotherms are displayed in Table 2. On the basis of the correlation coefficients (R^2), the Langmuir model gave a value >0.99, demonstrating that the adsorption of Cd(II) onto NaS-MS can be better described by the Langmuir model. This result indicates that the carboxyl groups of succinate are equivalent and all the adsorption sites are homogeneously distributed over the external and porous surfaces of MS.

In addition, the R_L values in this study vary between 0.0067 and 0.0636, which illustrate a favorable adsorption of Cd(II) by NaS-MS. On the other hand, the value of $1/n$ was less than 1, indicative of high adsorption intensity.

The adsorption capacity of NaS-MS for Cd(II) adsorption from Langmuir isotherm model is compared to those of other succinylated agriculture wastes so far reported in the literature.

Mercerized cellulose and nanocellulose present better adsorption efficiencies than NaS-MS (Table 3). However, when evaluating candidates for practical applications, the price of starting materials should be taken into consideration. The generation of mercerized cellulose and nanocellulose involves either time-consuming or high-cost procedures. The adsorbent used in this study is both economical and has a high sorption capacity, thereby making it a suitable adsorbent for the removal of Cd(II) from an aqueous solution.

Table 2
Parameters for the adsorption of Cd(II) by NaS-MS according to Langmuir and Freundlich isotherm models (original pH 5.8, adsorbent dose = 1 g L^{-1}, T = 293 ± 2 K, t = 1.5 h).

Langmuir isotherm model				Freundlich isotherm model		
K_L (L mg^{-1})	Q_{max} (mg g^{-1})	R_L range	R^2	K_F (L mg^{-1})	$1/n$	R^2
0.3036	196.1	0.0067–0.0636	0.9988	85.88	0.1621	0.8144

Table 3
Comparison of the Q_{max} of Cd(II) by succinylated agriculture wastes.

Agriculture wastes	Q_{max} (mg g^{-1})	Ref.
Cellulose	164	Gurgel, Júnior, Gil, and Gil (2008)
Mercerized cellulose	250	Gurgel et al. (2008)
Olive stone	200	Aziz et al. (2009)
Pineapple peel	93.5	Hu et al. (2010)
Sugarcane bagasse	196	Jr et al. (2007)
Filter acid cellulose	185.2	Belhalfaoui et al. (2009)
Mercerized nanocellulose	219.6	Hokkanen, Repo, and Sillanpää (2013)
Maize straw	196.1	This work

3.3.7. Thermodynamic study

To estimate the effect of temperature on the adsorption of Cd(II) onto NaS-MS, three basic thermodynamic parameters are studied: the Gibbs free energy of adsorption (ΔG), enthalpy change (ΔH) and entropy change(ΔS).

The Gibbs free energy of adsorption related to the equilibrium constant (K_C') is calculated from Eq. (11):

$$\Delta G = -RT \ln K_C' \quad (11)$$

where R is the universal gas constant (8.314 J mol^{-1} K^{-1}), T is the reaction temperature in K. K_C' is the distribution coefficient (versus the equilibrium concentration C_e and the amount of adsorption at equilibrium q_e).

The changes in enthalpy and entropy are determined using Eq. (12):

$$\Delta G = \Delta H - T\Delta S \quad (12)$$

The values of ΔH and ΔS are obtained from the slope and intercept of the plots of ΔG versus T.

The thermodynamic parameters are listed in Table S3.

As shown in Table S2, the adsorption capacity of Cd(II) does not vary significantly with the increase in temperature, indicating that the adsorption is not influenced by temperature. The observed negative values of ΔG at each temperature indicate that the adsorption of Cd(II) onto NaS-MS is spontaneous and Cd(II) has a high affinity for NaS-MS. Furthermore, the value of ΔG decreases with increase in temperature, suggesting that the adsorption is more efficient at high temperatures. The positive values of ΔH illustrate the endothermic nature of adsorption; hence, the number of ions adsorbed at equilibrium is higher at higher temperatures. The positive value of ΔS confirms an increase in the randomness at the solid–solution interface during the adsorption of Cd(II); this suggests that Cd(II) replaces the water molecules previously adsorbed on the surface of adsorbent. The displaced water molecules gain more translation entropy than that lost by the adsorbate ions (Wang et al., 2005).

3.4. Regenerability and recovery

3.4.1. Regeneration study

Repeated usability of the exchanger is a critical parameter for practical applications in treatment of industrial effluent. Saturated NaCl solution offers mild conditions and does not destroy the sensitive cellulose structure or the active sites (Belhalfaoui et al., 2009), and is therefore suitable as the desorption solution. The results from five replicates of adsorption–desorption are shown in Fig. S4. Mere 5.7% decrease in the adsorption capacity after five cycles underscores the reusability of the adsorbent. The mechanism of desorption is illustrated in Section 3.5.

3.4.2. Recovery of Cd(II) as its oxide

Since the adsorbent is modified carbohydrate polymer, it can disintegrate at a high temperature (873 K) leaving the oxide of Cd(II) as the residue. It is reddish brown powder and its structure is confirmed by XRD (Fig. S5). In our study, 7727 mg of Cd(II) is adsorbed and ~7486 mg of it is recovered, thus, the recovery is ~97%.

3.5. Adsorption mechanism analysis

It is necessary to investigate the dynamic model and sorption capacity of the maize straw due to the complex structure of the raw material. As shown in Fig. S6, its adsorption kinetics follows the pseudo-first-order kinetics and Q_{max} value by MS is only 35.7 mg g^{-1}, which is much lower than that of NaS-MS. The low adsorption capacity of MS agrees with the phenomena observed in the biosorption of cadmium(II) onto rice husk (Kumar, Ramakrishnan, Kirupha, & Sivanesan, 2010).The increase in sorption efficiency may be ascribed to the addition of succinate groups (Goyal & Srivastava, 2009). FTIR spectra of NaS-MS before and after adsorption are compared and shown in Fig. S7. Before adsorption the carboxylate ions give rise to two bands at 1592 and 1424 cm^{-1} which correspond to strong asymmetrical and symmetrical stretching bands, respectively. After contacting with Cd(II) solution, the band at 1592 cm^{-1} exhibits the evidence shift to a lower band at 1554 cm^{-1} while the peak at 1424 cm^{-1} shifts to 1427 cm^{-1}. These shifts demonstrate the complexation of carbonyl groups by deactive coordination (Fourest & Volesley, 1996). The difference ($\Delta\nu$) between $\nu_{asym}(COO^-)$ and $\nu_{sym}(COO^-)$ reflects the nature of the coordination status. Fuks, Filipiuk, and Majdan (2006) reported that bidentate chelating complexes exhibited a lower Δ ($\Delta_{complex} \ll \Delta_{Na\ salt}$); while monodentate complexes presented

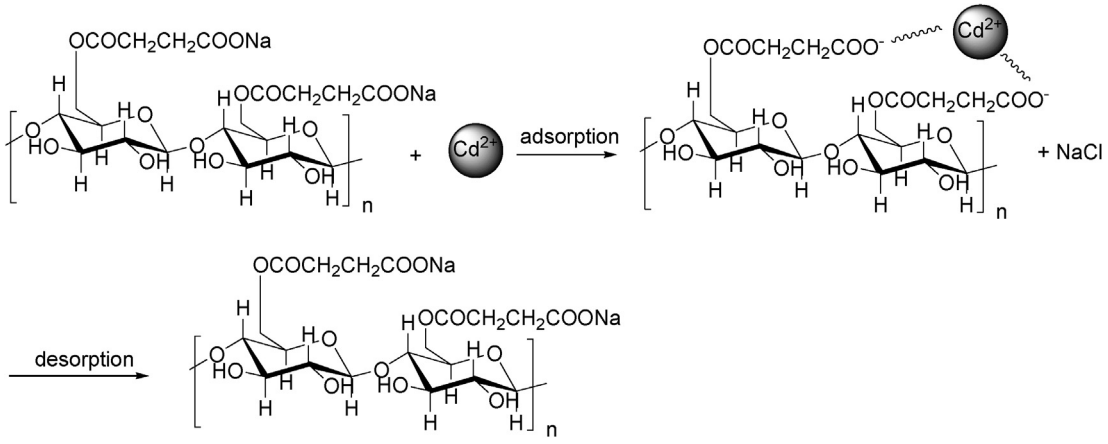

Fig. 7. The mechanism of adsorption and desorption of Cd(II) on the adsorbent.

a higher Δ ($\Delta_{complex} \gg \Delta_{Na\ salt}$). The distances for NaS-MS, cadmium-loaded S-MS are 168 and 127 cm^{-1} respectively. Therefore, Cd(II) binding with the carboxyl groups forms a bidentate chelating structure. Additionally, the Δ change indicates more involvement of carboxyl groups forming complexes with metal ions (Liu et al., 2011). The mechanism of adsorption and desorption is further investigated by SEM-EDX technique. As shown in Fig. S8, EDX analyses show that atomic percentages of sodium ion on MS and S-MS are 0.14% and 0%, respectively. The result demonstrates that sodium ion is separated from the raw material by succinoylation. After deprotonated by Na_2CO_3 solution, atomic percentage of Na is 4.58% which means S-MS can be converted into its sodic counterpart NaS-MS. After Cd(II) loaded, atomic percentages of Na and Cd are 0% and 2.75%, respectively. Cd(II) is substitute for all the sodium ions and atomic percentage of Na on NaS-MS is nearly as twice as adsorbed cadmium. The data illustrate that two succinate groups are involved in binding with one cadmium ion to form a bidentate chelating structure, which is also corroborated by FTIR spectra. The succinate groups' content (4.2 mmol g^{-1}) is twice more than the sorbed amount of cadmium (196.1 mg g^{-1}, i.e., 1.7 mmol g^{-1}) because the data obtained from EDX are semi-quantitative. After regenerated in NaCl solution, the atomic percentages of Na and Cd are 4.12% and 0.19%, respectively. Almost all the adsorbed cadmium ions are replaced by sodium ions, which is attributed to the ion exchange mechanism of Cd(II) by sodium ions. Fig. 7 illustrates the mechanism for Cd(II) adsorption and desorption in detail.

4. Conclusion

A novel adsorbent (NaS-MS) was successfully prepared from maize straw and exhibited a high Cd(II) adsorption capacity. Optimum removal occurred in initial pH range 4.0–7.0. The adsorption rate of Cd(II) on NaS-MS was very fast because of the low activation energy. The experimental data were described by the Langmuir isotherm with a maximum adsorption capacity of 196.1 mg g^{-1} at 293 K. Thermodynamic data indicated that the adsorption process was endothermic and spontaneous. NaS-MS can be fully regenerated for five cycles and a 97% recovery of the adsorbed Cd(II) as its oxide was possible. The mechanism studies confirmed that the adsorption process of Cd(II) on NaS-MS was a complicated process, which ion-exchange is the principal mechanism during adsorption and desorption. The Cd(II) adsorption capacity would be disturbed by other cations such as Zn(II), which is our ongoing research work concerning competitive adsorption.

Acknowledgements

This work was financially supported by the Educational Commission of Liaoning Province of China (No. L2013219) and the Youth Foundation of Dalian Polytechnic University (No. QNJJ201301).

Appendix A. Supplementary data

Supplementary data associated with this article can be found, in the online version, at http://dx.doi.org/10.1016/j.carbpol.2014.08.041.

References

Abou-Mesalam, M. M. (2003). Sorption kinetics of copper, zinc, cadmium and nickel ions on synthesized silico-antimonate ion exchanger. *Colloids and Surfaces A: Physicochemical and Engineering Aspects*, *225*(1–3), 85–94.

Aksu, Z. (2002). Determination of the equilibrium, kinetic and thermodynamic parameters of the batch biosorption of nickel(II) ions onto *Chlorella vulgaris*. *Process Biochemistry*, *38*, 89–99.

Aziz, A., Elandaloussi, E. H., Belhalfaoui, B., Ouali, M. S., & Ménorval, L. C. D. (2009). Efficiency of succinylated-olive stone biosorbent on the removal of cadmium ions from aqueous solutions. *Colloids and Surfaces B: Biointerfaces*, *73*(2), 192–198.

Baral, S. S., Das, S. N., Chaudhury, G. R., Swamy, Y. V., & Rath, P. (2008). Adsorption of Cr(VI) using thermally activated weed *Salvinia cucullata*. *Chemical Engineering Journal*, *139*(2), 245–255.

Belhalfaoui, B., Aziz, A., Elandaloussi, E. H., Ouali, M. S., & Ménorval, L. C. D. (2009). Succinate-bonded cellulose: A regenerable and powerful sorbent for cadmium-removal from spiked high-hardness groundwater. *Journal of Hazardous Materials*, *169*(1–3), 831–837.

Bhattacharyya, K. G., & Sharma, A. (2004). Adsorption of Pb(II) from aqueous solution by *Azadirachta indica* (neem) leaf powder. *Journal of Hazardous Materials*, *113*(1–3), 97–109.

Çay, S., Uyanık, A., & Özaşık, A. (2004). Single and binary component adsorption of copper(II) and cadmium(II) from aqueous solutions using tea-industry waste. *Separation and Purification Technology*, *38*(3), 273–280.

Chadlia, A., Mohamed, K., Najah, L., & Farouk, M. M. (2009). Preparation and characterization of new succinic anhydride grafted posidonia for the removal of organic and inorganic pollutants. *Journal of Hazardous Materials*, *172*(2–3), 1579–1590.

Chen, M., Zhao, J., & Xia, L. M. (2008). Enzymatic hydrolysis of maize straw polysaccharides for the production of reducing sugars. *Carbohydrate Polymers*, *71*(3), 411–415.

Clave, E., François, J., Billon, L., Sèbe, G., Jéso, B. D., & Guimon, M. F. (2004). Crude and modified corncobs as complexing agents for water decontamination. *Journal of Applied Polymer Science*, *91*(2), 820–826.

Fourest, E., & Volesky, B. (1996). Contribution of sulfonate groups and alginate to heavy metal biosorption by the dry biomass of *Sargassum fluitans*. *Environmental Science & Technology*, *30*(1), 277–282.

Fuks, L., Filipiuk, D., & Majdan, M. (2006). Transition metal complexes with alginate biosorbent. *Journal of Molecular Structure*, *792–793*, 104–109.

Goyal, P., & Srivastava, S. (2009). Characterization of novel *Zea mays* based biomaterial designed for toxic metals biosorption. *Journal of Hazardous Materials*, *172*(2–3), 1206–1211.

Gurgel, L. V. A., Júnior, O. K., Gil, R. P. F., & Gil, L. F. (2008). Adsorption of Cu(II), Cd(II) and Pb(II) from aqueous single metal solutions by cellulose and mercerized cellulose chemically modified with succinic anhydride. *Bioresource Technology*, *99*(8), 3077–3083.

Gusmão, K. A. G., Gurgel, L. V. A., Melo, T. M. S., & Gil, L. F. (2012). Application of succinylated sugarcane bagasse as adsorbent to remove methylene blue and gentian violet from aqueous solutions – Kinetic and equilibrium studies. *Dyes and Pigments*, *92*(3), 967–974.

Hokkanen, S., Repo, E., & Sillanpää, M. (2013). Removal of heavy metals from aqueous solutions by succinic anhydride modified mercerized nanocellulose. *Chemical Engineering Journal*, *223*, 40–47.

Hu, X. Y., Zhao, M. M., & Huang, H. H. (2010). Modification of pineapple peel fiber as metal ion adsorbent through reaction with succinic anhydride in pyridine and dimethyl sulfoxide solvents. *Water Environment Research*, *82*(8), 733–741.

Jr, O. K., Gurgel, L. V. A., Melo, J. C. P., Botaro, V. R., Melo, T. M. S., Gil, R. P. F., et al. (2007). Adsorption of heavy metal ion from aqueous single metal solution by chemically modified sugarcane bagasse. *Bioresource Technology*, *98*(6), 1291–1297.

Kalia, S., Kaith, B. S., & Kaur, I. (2009). Pretreatments of natural fibers and their application as reinforcing material in polymer composites – A review. *Polymer Engnieering and Science*, *49*, 1253–1272.

Kaušpedienė, D., Snukiškis, J., & Gefenienė, A. (2003). Kinetics of cadmium(II) sorption by an iminodiacetic ion exchanger in the presence of a nonionic surfactant. *Desalination*, *154*(1), 67–77.

Khaled, A., Nemr, A. E., El-Sikaily, A., & Abdelwahab, O. (2009). Removal of direct N Blue-106 from artificial textile dye effluent using activated carbon from orange peel: Adsorption isotherm and kinetic studies. *Journal of Hazardous Materials*, *165*(1–3), 100–110.

Kiefer, E., Sigg, L., & Schosseler, P. (1997). Chemical and spectroscopic characterization of algae surface. *Environmental Science & Technology*, *31*, 759–764.

Kumar, P. S., Ramakrishnan, K., Kirupha, S. D., & Sivanesan, S. (2010). Thermodynamic and kinetic studies of cadmium adsorption from aqueous solution onto rice husk. *Brazilian Journal of Chemical Engineering*, *27*, 347–355.

Lehrfeld, J. (1996). Conversion of agricultural residues into cation exchange materials. *Journal of Applied Polymer Science*, *61*(2), 2099–2105.

Liu, C. F., Sun, R. C., Qin, M. H., Zhang, A. P., Ren, J. L., Ye, J., et al. (2008). Succinoylation of sugarcane bagasse under ultrasound irradiation. *Bioresource Technology*, *99*(5), 1465–1473.

Liu, H. J., Yang, F., Zheng, Y. M., Kang, J., Qu, J. H., & Chen, J. P. (2011). Improvement of metal adsorption adsorption onto chitosan/*Sargassum* sp. composite sorbent by an innovative ion-imprint technology. *Water Research*, *45*(1), 145–154.

Liu, D. G., Zhu, Y., Li, Z. H., Tian, D. L., Chen, L., & Chen, P. (2013). Chitin nanofibrils for rapid and efficient removal of metal ions from water system. *Carbohydrate Polymers*, *98*(1), 483–489.

Macías-García, A., Gómez-Serrano, V., Alexandre-Franco, M. F., & Valenzuela-Calahorro, C. (2003). Adsorption of cadmium by sulphur dioxide treated activated carbon. *Journal of Hazardous Materials*, *103*(1–2), 141–152.

Malla, M. E., Alvarez, M. B., & Batistoni, D. A. (2002). Evaluation of sorption and desorption characteristics of cadmium, lead and zinc on Amberlite IRC-718 iminodiacetate chelating ion exchanger. *Talanta*, *57*(2), 277–287.

Ramakrishna, M., & Sulochana, N. (2009). Utilization of waste biomass for the removal of basic dye from water. *World Applied Science Journal*, *5*, 114–121.

Srivastava, V. C., Mall, I. D., & Mishra, I. M. (2008). Adsorption of toxic metal ions onto activated carbon: Study of sorption behaviour through characterization and kinetics. *Chemical Engineering and Processing: Process Intensification*, *47*(8), 1269–1280.

Vieira, A. P., Santana, S. A. A., Bezerra, C. W. B., Silva, H. A. S., de Melo, J. C. P., da Silva Filho, E. C., et al. (2010). Copper sorption from aqueous solutions and sugar cane spirits by chemically modified babassu coconut (*Orbignya speciosa*) mesocarp. *Chemical Engineering Journal*, *161*(1–2), 99–105.

Vimonses, V., Lei, S. M., Jin, B., Chow, C. W. K., & Saint, C. (2009). Adsorption of congo red by three Australian kaolins. *Applied Clay Science*, *43*(3–4), 465–472.

Wang, L., Zhang, J., Zhao, R., Li, C., Li, Y., & Zhang, C. L. (2010). Adsorption of basic dyes on activated carbon prepared from *Polygonum orientale* linn: Equilibrium, kinetic and thermodynamic studies. *Desalination*, *254*(1–3), 68–74.

Wang, S. G., Guo, X. Q., & Guo, Y. L. (2006). Chemical structure and pyrolysis properties of cornstalk lignin. *Journal of South China University of Technology (Natural Science Edition)*, *34*(3), 39–42.

Wang, Y. S., Xue, M., Zheng, X. H., Ji, B. M., Du, R., & Wang, Y. F. (2005). Effects of environmental factors on N_2O emission from and CH_4 uptake by the typical grasslands in the Inner Mongolia. *Chemosphere*, *58*(2), 205–215.

Weber, W. J., & Morris, J. C. (1963). Kinetics of adsorption on carbon from solution. *Journal of the Sanitary Engineering Division*, *89*(SA2), 31–59.

Zhang, J. M., Zhai, S. R., Li, S., Xiao, Z. Y., Song, Y., An, Q. D., et al. (2013). Pb(II) removal of Fe_3O_4@SiO_2-NH_2 core–shell nanomaterials prepared via a controllable sol–gel process. *Chemical Engineering Journal*, *215–216*, 461–471.